POLARIZATION LIFETIME IN AN ELECTRON STORAGE RING, AN ERGODIC APPROACH IN eRHIC EIC[*]

F. Méot, BNL C-AD, Upton, NY, USA

Abstract

Electron polarization in a storage ring is subject to two long-term effects: Sokolov-Ternov polarization and depolarization by diffusion. Over a long time scale this leads to an equilibrium state and, simulation-wise, can be highly CPU time and memory consuming. Simulations aimed at determining optimal ring storage energy in an electron-ion collider use to track thousand particle bunches, for a long time—yet still short compared to depolarization time scales, due to HPC limitations. Based on considerations of ergodicity of electron bunch dynamics in the presence of synchrotron radiation, tracking a single particle instead is investigated. This allows substantial saving in teh required HPC volume, "CPU-time × Memory-allocation". The concept is illustrated with polarization lifetime and equilibrium polarization simulations at the eRHIC electron-ion collider.

INTRODUCTION

The eRHIC installation is briefly described in Fig. 1 [1]. The 18 GeV eRHIC electron storage lattice used in the
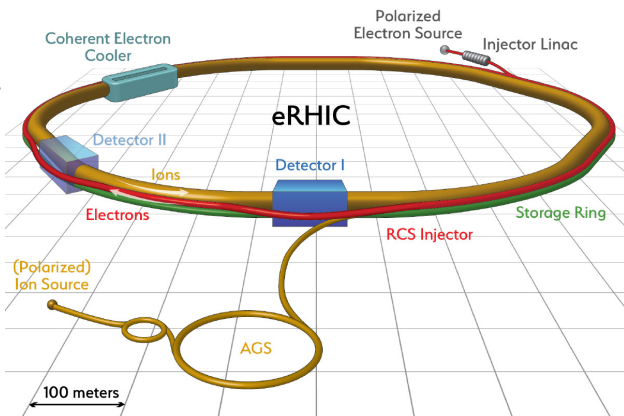

Figure 1: The eRHIC electron-ion collider complex, an 18 GeV–255 Gev/nucleon electron-ion collider installation.

present spin polarization simulations has been provided by S. Tepikian [1], optical parameter values relevant to the present simulations will be introduced in due place. The eRHIC lattice includes a double non-planar rotator system (Fig. 2) at the interaction point (IP), comprised of strong solenoids and series of bends, which allows to locally move the stable spin precession direction $\vec{n}_0$, from vertical in the arcs to longitudinal at the IP. In a defect-free ring, this region of off-vertical $\vec{n}_0$ is a major contribution to spin diffusion.

Bunches are injected in the storage ring with alternately up and down polarization, and replaced every 6 min in order
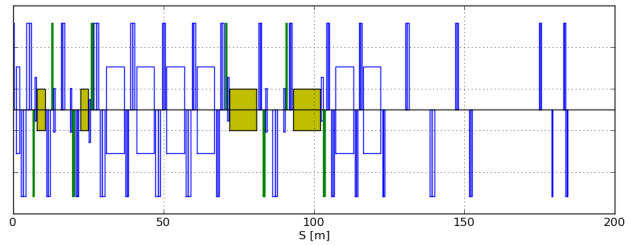
Figure 2: Half of the spin rotator system at eRHIC (the system is symmetric with respect to the IP, at the origin here). In green: solenoids.

to ensure an average polarization of 70% over the hundreds of bunches stored [1]. A proper lattice should maintain bunch depolarization below 20% (absolute) over the 6 min storage. The evolution of the polarization, from $P_0 = \pm 0.85$ at injection to P_{eq} at equilibrium (an asymptotic quantity to be determined), satisfies

$$P(t) = P_{eq}(1 - e^{-t/\tau_{eq}}) + P_0 e^{-t/\tau_{eq}}. \quad (1)$$

This results from (i) synchrotron-radiation (SR) self-polarization and (ii) polarization loss by diffusion, with time constant τ_D, such that

$$1/\tau_{eq} = 1/\tau_{SP} + 1/\tau_D \quad (2)$$

Sokolov-Ternov (ST) self polarization in a flat ring has a time constant $\tau_{ST[sec.]} \approx 99\rho_{[m]}^2 R_{[m]}/E_{[GeV]}^5$ [2], about 30 min at eRHIC at 18 GeV, 10 hrs at 10 GeV, with asymptotic value $P_{ST} = 92.4\%$; the asymptotic self-polarization is taken instead $P_{SP} = 90\%$ here to account for the non-planar spin rotator, and with time constant τ_{SP}, such that [2]

$$P_{eq} = P_{SP} \times \tau_{eq}/\tau_{SP}. \quad (3)$$

The goal in tracking spin motion is (i) to validate a ring design, including preservation of polarization under the effect of defects, corrections, etc. and (ii) to determine an optimal working point $a\gamma_{ref}$ ($a = 1.15965 \times 10^{-3}$ is the electron anomalous magnetic moment).

In the following, a method based on single-particle tracking is discussed. First, basic aspects of the stochasticity of particle and spin motions are recalled. Then tracking outcomes are displayed and the single-particle method is discussed.

The numerical simulations discussed in this paper have strongly benefited from NERSC means and environment [3].

STOCHASTIC MOTION

The dynamical system of a high energy stored electron bunch at equilibrium is ergodic: over a long time interval, trajectories in the system cover all parts of the 6D phase space.

Time averages over one or more trajectories are equivalent to phase space averages,

$$\lim_{T \to \infty} \int_{t_0}^{t_0+T} f(\vec{X}(t))dt = \int f(\vec{X})\rho(\vec{X})d^N \vec{X} \Big|_{\text{time}=t} . \quad (4)$$

For all three motions, transverse and longitudinal, the evolution of the bunch emittance with time, t, satisfies

$$\overline{\epsilon}_n(t) = \epsilon_{n,\text{eq}} \left(1 - e^{-t/\tau_n}\right) + \epsilon_{n,i}\, e^{-t/\tau_n} \quad (5)$$

(n stands for x, y, or l) with $\epsilon_{n,i}$ and $\epsilon_{n,\text{eq}}$ respectively the starting and equilibrium emittances, $\tau_n = \dfrac{T_{\text{rev}}\, E_s}{U_s\, J_n}$ the damping time constant. $J_{n=x,y,l}$ are the partition numbers, $J_x + J_y + J_l = 4$, $J_l \approx 2$. Equation (5) indicates that after a few damping times, the bunch dynamical system can be considered at equilibrium, bunch emittances have reached their asymptotic values. In the following $\tau_{\text{SR}} = \tau_x \approx \tau_y$ denotes the transverse damping time constant.

At 18 GeV the energy loss amounts to 38.7 MeV/turn (a result from prior tracking of a 2000 particle bunch with Monte Carlo SR), thus the damping time amounts to $\tau_{\text{SR}} = 18_{\text{GeV}}/38.7_{\text{MeV/turn}} = 465$ turns, 6 ms.

Figures 3 and 4 display the stochastic motion of a single particle over $10^3 \tau_{\text{SR}}$ and by comparison the instantaneous horizontal and vertical phase spaces of a 10^3-electron bunch observed at $time = 10^3 \tau_{\text{SR}}$. In this example, statistical variable values such as *rms* coordinates, emittances, either single particle projected over a long tracking time, or multiparticle at time $t = 10^3 \tau_{\text{SR}}$, resulting from both methods, essentially satisfy Eq. (4). Over a sufficiently long time interval, an electron has explored the all 6D phase-space, which is a necessary condition for ergodicity to be satisfied.

Out of equilibrium, $\vec{X}(t) - \underline{X}(t)$ can be taken as the statistical vaiable, with $\underline{X}(t)$ the average value. $\underline{X}(t)$ can be determined from a fit using the theoretical damping, for instance in the single particle case, see below. Spin motion is not at equilibrium, the polarization decays with time, fast in resonant conditions. Both the decay time constant and the asymptotic polarization are zero on the resonance, as $\tau_{\text{eq}} \sim \delta^2 \times \tau_{\text{SP}}$, $P_{\text{eq}} \sim \delta \times P_{\text{SP}}$, with $\delta = a\gamma_{\text{Res.}} - a\gamma$ the distance to the resonance [2, p. 125]. Figure 5 displays typical stochastic spin motion in eRHIC storage ring at 18 GeV. In a similar way that τ_{SR} can be obtained from the observation of the damped motion of a single electron far from equilibrium, τ_D can be obtained from long enough observation of spin motion.

POLARIZATION

In order to assess polarization properties of a storage ring depending on its energy setting, spin tracking simulations are performed over an ensemble of $a\gamma_{\text{ref}}$ rings covering some $a\Delta\gamma_{\text{ref}} < 1$ range of interest. In these hypothesis, all these rings have the same optics: bend strengths $1/\rho$, focusing strengths $G/B\rho$, chromaticities, etc., are unchanged, what changes is the energy $a\gamma_{\text{ref}}$ at which each ring is run.
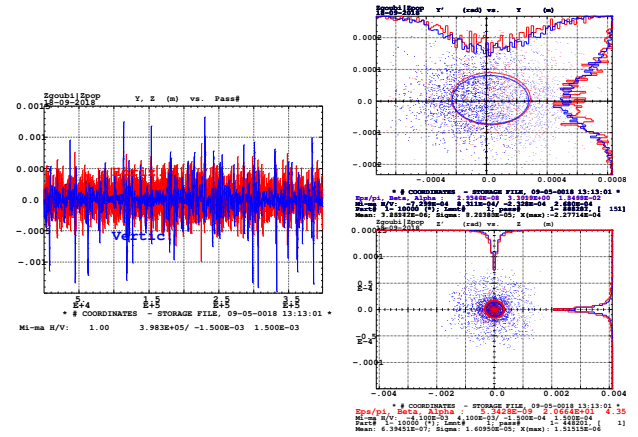

Figure 3: Left: transverse particle excursion, over time interval $t/\tau_{\text{SR}} : 1 \to 10^3$ (450,000 turns about). Right: transverse phase spaces, matching ellipses and histograms; blue: projection of the single particle motion of the left plot; red: for comparison, case of a 10^3 particle bunch, observed at time $t = 10^3 \tau_{\text{SR}}$. Note that the ϵ_y/ϵ_x ratio represents a 27% coupling, of which the source is the spin rotator in IR6 which includes solenoids (Fig. 2).
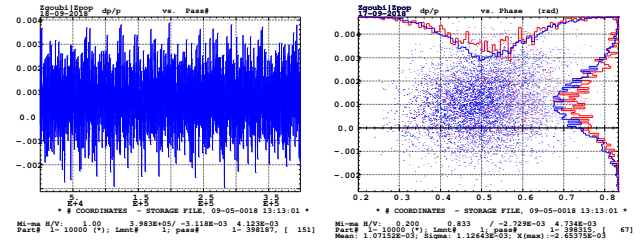

Figure 4: Left: stochastic energy excursion over time interval $t/\tau_{\text{SR}} : 1 \to 10^3$. $\sigma_{\delta p/p} = 1.14 \times 10^{-3}$. Right: longitudinal phase space; red: case of a 10^3 particle bunch observed at $t = 10^3 \tau_{\text{SR}}$; $\sigma_{\delta p/p} = 1.13 \times 10^{-3}$; blue: projection of the multiturn single particle motion of Fig. 4.

Particles are all launched with their initial spin direction parallel to the local nominal stable spin precession direction $\vec{n}_0$ (*i.e.*, longitudinal if the origin is taken at IP6, vertical at IP8). Spin tracking only starts after 10 damping times about (5,000 turns) when the bunch has reached its equilibrium emittance. If the motion happens to neighbor a depolarizing resonance, spin will tilt away from the nominal direction toward possibly large angles depending on the strength of/distance to the resonance (in the absence of SR and at constant energy, the spin would steadily rotate around the local tilted $\vec{n}_\delta$). Away from any resonance, the spin is expected to only be subject to slow diffusion.

The single particle "depolarization landscape" is expected to look as shown in Fig. 6, obtained in HERA-e conditions, which include a spin rotator which introduces strong depolarization in the $a\gamma$ = integer regions. Single particle tracking here yields Figure 7 (18 GeV) and Fig. 8 (10 GeV), which appears qualitatively similar to DESY simulation outcomes, Fig. 6. This is the outcome of the tracking, over a time
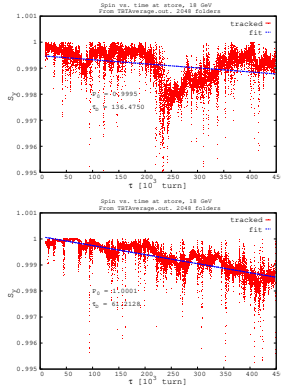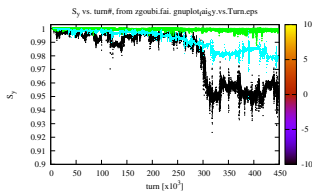
Figure 5: Left: stochastic spin motion observed at IP8 ($\vec{n}_0$ vertical there), single particle, a few different cases of ring rigidity settings in the 18 GeV region. Right: monitor individual spins, a linear regression on $P/P_0 = \exp(-t/\tau_D) \approx 1 - t/\tau_D$ provides the diffusion time constant τ_D.
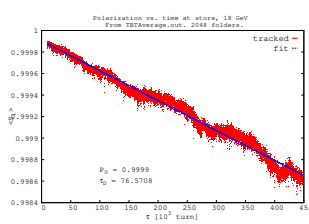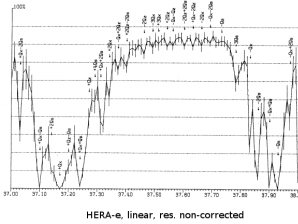

Figure 6: Left: asymptotic polarization at HERA, using SITROS [4]. This graph was produced by tracking bunches of a few hundred polarized electrons, including Monte Carlo SR, over a few SR damping times, for a series of evenly spaced ring rigidity values over an $a\Delta\gamma = 1$ interval ($37 \leq a\gamma \leq 38$). Each $a\gamma$ value represents a particular operation rigidity of the ring, however with unchanged optics. Right, obtained from the present eRHIC simulations: turn-by-turn average spin value over the complete bunch population yields the self-polarization time constant, from what the asymptotic polarization, similarly to the representation in the left plot, can be drawn (average over just a few particles is shown here).

interval $[0, t]$, of a single particle in each one of 1024 (or 2048) rings, all operated with the same optics but with each its particular operation energy $a\gamma_{\mathrm{ref}}$. These distributions feature similar topology, at both timings. Zooming in on any reduced $a\Delta\gamma_{\mathrm{ref}}$ interval also shows a similar spin distribution (sort of "fractal"). The energy excursion over that time interval $[0, t]$ is displayed in Fig. 9. Note a property that will be referred to later: the equilibrium energy spread is $\sigma_E \approx 10^{-3}E$ at 18 GeV, or an extent $\sigma_{a\gamma} \approx 0.04$, thus the beam covers ≈ 40 (80) bins of a 1024 (2048) bin $a\Delta\gamma_{\mathrm{ref}} = 1$ interval.

Spin diffusion has to be a slow process for a lattice to be viable, in particular this cannot be the case if, during its energy excursion, a particle neighbors (is within a few resonance strengths from) a depolarizing spin resonance ($\nu_s \pm l\nu_x \pm m\nu_y \pm n\nu_l =$ integer). In such case, the de-

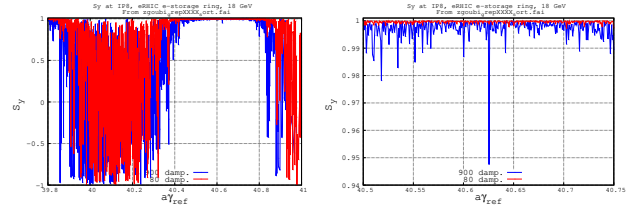Figure 7: Spin rotation landscape (a photo of the spins, $S_l(a\gamma_{\mathrm{ref}})|_{\mathrm{time}=t}$ at IP8 where $\vec{n}_0$ is vertical), at either (red) $t = 80\tau_{\mathrm{SR}}$ (4×10^4 turns) or (blue) $t = 900\tau_{\mathrm{SR}}$ (4.5×10^5 turns or 5 s). Left: the 2048 rings tracked cover over a $a\Delta\gamma = 1.2$ interval, encompassing integer $a\gamma_{\mathrm{ref}}$ values where full spin flip is observed, as expected. Right: a zoom in on a reduced $40.5 < a\Delta\gamma_{\mathrm{ref}} < 40.75$ interval; no strong resonances in that region instead, and spins remain close to $S_y = 1^-$.
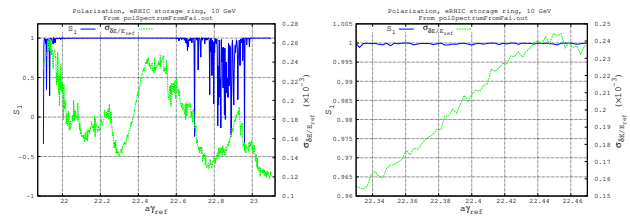

Figure 8: Spin rotation landscape (a photo of the spins, $S_l(a\gamma_{\mathrm{ref}})|_{\mathrm{time}=t}$ at IP6 where $\vec{n}_0$ is longitudinal), at 160 SR damping times ($\approx 5 \times 10^5$ turns). The right and left plots differ by the $a\Delta\gamma$ interval width. Integer $a\gamma_{\mathrm{ref}}$ regions show full spin flip as expected. In the reduced $22.33 < a\gamma_{\mathrm{ref}} < 22.47$ region no strong resonance is observed, spins remain close to $S_y = 1^-$. The right vertical scale in both plots is the *rms* width of the energy interval explored by a particle during the tracking.

polarization *is not* slow (the orientation of the spin vector changes substantially during the tracking: the vertical spin component S_y moves towards $S_y = -1$ in the present representation, Fig. 5). Thus, the working point of concern, $a\gamma_{\mathrm{ref}}$ near resonance, is not optimal. *A contrario*, observing only slow change in the spin vector means absence of harmful resonance in the energy interval that the particle spans due to SR, and potentially a viable working point.

Diffusion Time Constant

Spin tracking here does not include the self-polarization process, it is assumed that τ_{SP} in Eq. (2) is obtained from the lattice. Thus, a bunch keeps depolarizing, due to diffusion, polarization tends toward $P_{\mathrm{eq}} = 0$ ($\tau_{\mathrm{SP}} = \infty$) with a time constant $\tau_D = \tau_{\mathrm{eq}}$.

In order to ensure the required polarization survival (70% on average over the ensemble of bunches in the ring, stored 6 min each) τ_D has to be sufficiently long compared to the store duration; this eliminates, for a viable rigidity setting of the ring, the regions $a\gamma_{\mathrm{ref}} < 40.45$ and > 40.75 in Fig. 7 (18 GeV), $a\gamma_{\mathrm{ref}} < 22$ and > 22.4 in Fig. 8 (10 GeV). Finally, with τ_D much larger than the time interval covered by the tracking (of the order of seconds at best, whereas τ_D has to
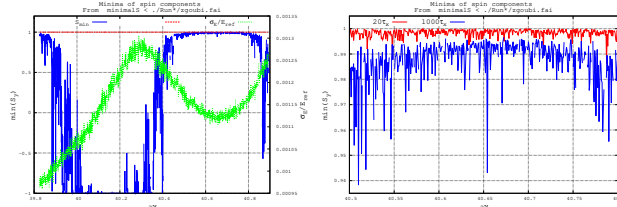
Figure 9: Left, blue curve: depolarization landscape $S_{y,\min}(a\gamma_{\text{ref}})|_{t\in[0,T]}$, over $39.8 < a\gamma_{\text{ref}} < 40.9$ (18 GeV region), observed at IP8 (nominal $\vec{n}_0$ is vertical there) at time $T = 10^3\tau_{\text{SR}}$. This is the smallest value of the projection of particle spin $\vec{S}$ on the vertical axis, reached over the time interval $[0,T]$. The right vertical scale (green curve) is the *rms* width of the energy interval explored by a particle during the tracking. Right: a zoom in on a reduced $40.5 < a\Delta\gamma_{\text{ref}} < 40.8$ interval, showing $S_{y,\min}(a\gamma_{\text{ref}})|_{t\in[0,T]}$ at (red) $T = 20\tau_{\text{SR}}$ (9500 turns) and (blue) $T = 1000\tau_{\text{SR}}$ (450,000 turns or 6 s).

amount to tens of minutes for a lattice to be viable), one can use

$$P(t)/P_0 = \exp(-\frac{t}{\tau_{\text{D}}}) \approx 1 - t/\tau_{\text{D}}. \qquad (6)$$

Single particle spin tracking data are displayed in Fig. 5, a fit of these data provides τ_{D}. From that τ_{eq} can be derived (Eq. (2)) yielding in turn P_{eq} (Eq. (3)) and $P(t = 6\,\text{min})$ (Eq. (1)).

In order to assess the method, in the following for simplicity, and P_{eq} being a sub-product, primary tracking outcomes are considered, namely, spin orientation or τ_{D} landscapes.

A METRIC

Typically, the energy dependence of particle spins over a $a\Delta\gamma_{\text{ref}}$ interval looks as shown in Figs. 7 and 8. A different criterion to quantify the depolarization could be instead, Fig. 9, the energy dependence of the minimal value that spins reached in the course of the tracking. This minimum may happen earlier in the tracking, as observed in Fig. 5, as spins oscillate around a given tilted local $\vec{n}_\delta$, as long as the latter does not change due to photon emission.

In order to allow comparisons between lattices a metric is required. However, Figs. 7 and 8 styles of data do not lend themselves to straightforward comparisons, essentially due to the stochastic aspect. A couple of different possibilities are assessed here instead, based on sliding averaging.

Spin

A sliding average of the data of Fig. 7, with a small sliding interval $a\delta\gamma_{\text{ref}}$ (a few particles / bins), namely

$$\langle S_y \rangle_N(a\gamma_{\text{ref},\frac{N}{2}}) = \frac{1}{N} \sum_{i}^{i+N-1} S_y(a\gamma_{\text{ref},i}), \qquad (7)$$

greatly smooths the fluctuations, as observed in Fig. 10. The local excursion of S_y over a small $\delta\gamma_{\text{ref}}$ interval in the optimal region ($P_f/P_i \approx 0.9983$) are grossly below $\pm 2 \times 10^{-4}$. This

corresponds to a fluctuation of τ_{D} of less than $\pm 7\,\text{min}$ around an average $\approx 60\,\text{min}$, $\approx \pm 10\%$ relative, a good first approach. This can be further improved by increasing the number of bins, for instance, once determined that the region $40.6 < a\gamma_{\text{ref}} < 40.7$ is viable, the computation can be reiterated.
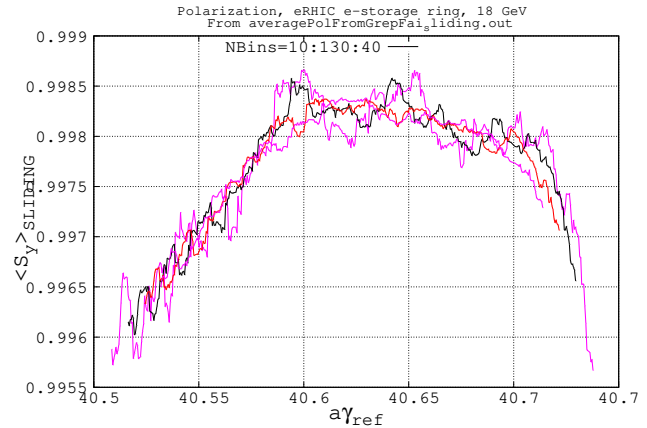

Figure 10: Derived from Fig. 7, by applying a sliding average (Eq. (7)). The four curves differ by the sampling: average over N= either 10, 50, 90 or 130 $a\delta\gamma_{\text{ref}}$ samples, centered at given $a\gamma_{\text{ref}}$ In the present conditions, the distribution converges when increasing the number of samples, N, i.e., the width of the sliding interval, $[a\delta\gamma_{\text{ref},i}, a\delta\gamma_{\text{ref},i+N}]$.

Why allow a sliding average:

1. with the present extent $a\Delta\gamma_{\text{ref}} \approx 1$ covered in 1024 bins (or 2048), the energy extent of the bunch $\sigma_{\gamma_{\text{ref}}}/\gamma_{\text{ref}} \approx 10^{-3}$ or $a\delta\gamma_{\text{ref}} = 0.04$, covers about 40 (or 80) bins,

2. thus, a set of a few neighboring bins almost belong in the same ring, averaging over a few bins is not so different from averaging over a few particles in the same bin,

3. in any case a possible strong, nearby resonance would cause a dip in the distribution, indicating a non viable $a\delta\gamma_{\text{ref}} = 1$ region, which has to be avoided.

The strong smoothing effect of a sliding average suggest to apply it directly to the final spin distribution, this is done in Fig. 10, case of a $\Delta\gamma$: $40.4 \to 40.9$ interval covered in 1024 bins. In the present conditions, this series converges when increasing the width of the sliding interval $[a\delta\gamma_{\text{ref},i}, a\delta\gamma_{\text{ref},i+N}]$. At some point however, increasing the sliding interval would cause it to reach $a\gamma_{\text{ref}}$ regions where the fluctuations change in a sensible manner (as in Fig. 7, left), for instance featuring a different average, or including high amplitude spikes, so abruptly changing the sum of the series, however the eRHIC lattices of interest have to satisfy $< S_y > (a\gamma_{\text{ref}}) \approx 1$, which prohibits such changes. In the present case of 1024 ring samples over $\Delta\gamma$: $40.4 \to 40.9$, $N = 40$ appears appropriate; this is a sliding window of full width $a\Delta\gamma_{\text{ref}} = 40 \times (40.9 - 40.4)/1024 \approx 0.02$. Figure 10

MOPAF03

confirms that, with the 40.59–40.63 interval yielding a final $\tau_D \approx 55\%$ within about ±5% of convergence values for both 40.60–40.62 and 40.56–40.66 sliding windows. It may also be thought of increasing the bins density in the $a\gamma_{ref}$ of interest to obtain a better homogeneous distribution.

Diffusion Time Constant

The diffusion time constant is derived from single particle motion using a linear regression (Eq. (6)), an illustration can be found in Fig. 5 (right). Applying to each of the 2048 rings over the $a\Delta\gamma_{ref}$ interval, yields the scan in Fig. 11. Tracking over several SR damping times is needed to draw τ_D from individual spin motion, It can be seen in Fig. 11 that, in the region of τ_D values of interest the statistics over 80, 160 and $10^3\tau_{SR}$ superimpose. This indicates that the required tracking time is comparable with that needed to determine τ_{SR} from particle motion, which is a few tens of damping times or less. On the other hand, in case the strong fluctuations of the spin would cause too strong a dependence of the τ_{SR} value (from the fit) on the fit sample, rather than increasing the damping time a possibility is instead to launch a few particles per ring: the smoothing effect is immediate, this can be seen by comparison of the spin motion in Fig. 5 (right) and the averaging over a few particles in Fig. 6 (right). These considerations matter as to the interest of the single particle method, this is discussed in the next section.

Again a sliding average, applied to the data of Fig. 11, greatly smooths the fluctuations, as observed in Fig. 12. The distance between τ_D distributions can be derived from Fig. 12 type of data, which are thus usable for comparing polarization performances of different versions of the eRHIC e-storage ring.

SUMMARY

Assume similar resolution using both methods, "HPC-Hungry" and "Ergodic", namely, the same number of reference rings, nRings, over the same interval $a\Delta\gamma$.

In the present hypotheses (eRHIC lattice, energy, etc.):

- first method: the HPC volume is nRings $\times 10^3$ [particles/bunch] $\times$ a few τ_{SR},

- second method: the HPC volume is nRings $\times$ a few τ_{SR}.

This is a 3 orders of magnitude difference in the HPC volume. On the other hand, greater HPC volume translates in one or the other of, longer queues, longer computing time, more processors, greater volume of I/Os, larger data analysis HPC volume.

It remains to determine how close the single particle method can get to the accuracy of the bunch method (an ongoing work). However it already appears an efficient first approach to the diffusion time constant, in view of qualifying an evolution of a lattice design, the efficiency of error correction and other spin matching schemes. Because it is faster it allows a greater reach (for instance in terms of
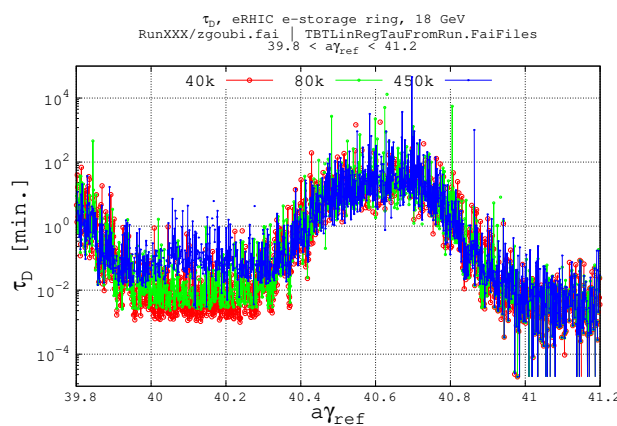
Figure 11: Energy scan of the diffusion time constant in the single particle tracking method. 2048 bins cover $a\Delta\gamma$: 39.8–41.2. τ_D values interpolated from 80 (red), 160 (green) and $10^3\tau_{SR}$ tracking.
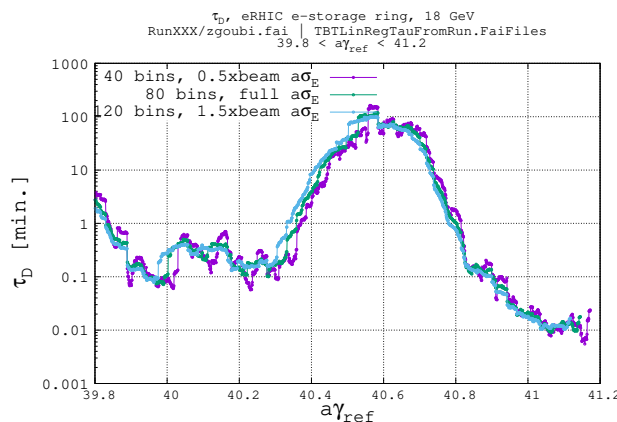

Figure 12: Sliding over energy scan of the diffusion time constant in the single particle tracking method. 2048 bins.

parameter space exploration) in machine simulations and design optimizations.

CONCLUSION

Obviously these results are very preliminary, they are essentially indications that the HPC volume could be reduced. More simulations are required, for further inspection, comparisons between the two methods, etc. Mathematical background and support is in order.

The simulations discussed here were performed on NERSC [3], using stepwise ray-tracing tools for spin motion accuracy [5, 6]. Electron dynamics and spin diffusion in the presence of Monte Carlo SR is a long installed and, needless to say, thoroughly benchmarked feature of the code [7].

ACKNOWLEDGEMENTS

REFERENCES

[1] eRHIC p-CDR, BNL, 2018.

[2] S.Y. Lee, *Spin dynamics and snakes in synchrotrons*, World Scientific, 1997.

[3] NERSC computing, `http://www.nersc.gov/`

[4] J. Kewisch, "Depolarisation der Elektronenspins in Speicherringen durch nichtlineare Spin-Bahn-Kopplung", DESY 85-109, Okt. 1985.

[5] `https://zgoubi.sourceforge.io/ZGOUBI_DOCS/Zgoubi.pdf`

[6] `https://www.osti.gov/scitech/biblio/1062013-zgoubi-users-guide`

[7] F. Méot, "Simulation of radiation damping in rings, using stepwise ray-tracing methods", *JINST*, vol. 10, pp. T06006, 2015.